# Shape-dependent depinning of a domain wall by a magnetic field and a spin-polarized current

N. Logoboy,[1,2,*] B. Ya. Shapiro,[1] and E. B. Sonin[2]
[1]*Institute of Superconductivity, Department of Physics, Bar-Ilan University, 52900 Ramat Gan, Israel*
[2]*The Racah Institute of Physics, The Hebrew University of Jerusalem, 91904 Jerusalem, Israel*
(Received 21 June 2010; revised manuscript received 22 August 2010; published 13 September 2010)

The effect of sample shape on the depinning of the domain-wall (DW) driven by an applied magnetic field or a spin-polarized current is studied theoretically. The shape effect resulting from the modulation of the sample width (geometric pinning) can essentially affect the DW depinning. We found a good agreement between the ratios of the critical values of the magnetic field and the spin-polarized current predicted by the theory and measured in the experiment.

DOI: 10.1103/PhysRevB.82.094419 PACS number(s): 72.30.+q, 75.60.Ch, 75.70.Ak, 85.75.−d

## I. INTRODUCTION

During the last years an immense interest in current-driven domain-wall (DW) motion in thin magnetic films, nanotubes, and point contacts has been initialized by possible applications in spintronic device technology (see, e.g., Refs. 1 and 2, and references therein). These devices are expected to be highly efficient, fast, and consuming less energy. They possess such important features as nonvolatility, portability, and capability of simultaneous data storage and processing. A manipulation of magnetization by spin-polarized current predicted by Berger for nonuniform ferromagnets[3] and Slonczewski for multilayered ferromagnetic structures[4] has attracted the attention of physical community during last decade and gained further development in Refs. 5–12.

The problem of DW motion under another driving force, applied magnetic field, was addressed in late 1970s in connection to possible application in memory storage devices (see, e.g., Ref. 13). In pioneering work of Schryer and Walker[14] it was shown the existence of an instability in the laminar movement of the DW. These early results can actually serve as a reference for the studies of spin-polarized current-driven DW motion. In particular, it is well established now that for DW driven by magnetic field (or spin-polarized current, or both) there exists a critical value of driving parameter(s) which corresponds to maximum velocity of the DW (Walker velocity[14]). Thus, the DW dynamics includes two distinct regimes, so-called subcritical (below the Walker breakdown) and supercritical (above the Walker breakdown) ones.[1,7] Below the Walker limit the overdamped transient response of the system to applied magnetic field follows by a steady state response while above the Walker limit the DW dynamics is oscillatory with nonzero average velocity.

In the case of field-driven DW motion the exact stationary wave solution in subcritical regime was obtained more than half-century ago by Walker.[15] Analytical results of Bourne[16] reproduced a velocity profile in full range of magnetic field confirming numerical simulations of Slonczewski in supercritical regime.[17]

Modern fabricated logic elements based on manipulation of the DWs are represented by a complex networks of nanowires, which can form three-dimensional memory storage structure, e.g., a racetrack device that comprises an array of magnetic nanowires arranged horizontally or vertically on a silicon chip.[18] The spacing between consecutive DWs is controlled by pinning sites fabricated by patterning notches along the edges of the track or modulating the track's size and material properties. Being a necessary component of the logic elements, the pinning sites define the bit length and provide the DWs stability against external perturbations, such as thermal fluctuations or stray magnetic fields from nearby racetracks. The variation in the nanowire geometry creates the pinning potential for the DW and may essentially affect the properties of the wall. According to Bruno,[19] at a very small characteristic length of a constriction separating two wider regions the width of the DW is given by this characteristic length and does not depend on the magnetic anisotropy and stray field so that such a wall constitutes a new kind of the DW, besides the well-known Bloch and Néel walls. Geometrically induced pinning can be stronger than the pinning due to natural imperfections.[20] Therefore, the depinning field in nanostructures with constrictions can be adjusted over a wide range of values by changing the notch geometry.

The strength and width of pinning potential are crucial parameters in designing of memory devices with the low current consumption. The underlying origin of the depinning magnetic field, $H_c$, and threshold current, $J_c$, is extremely important. The case of imperfections of the material (existence of pinning centers or edge roughness) was considered in details by Tatara and Kohno[6] who showed that in a limit of weak pinning a threshold current is proportional to the hard-axis anisotropy while in opposite limit of strong pinning it is entirely determined by the strength and width of the pinning potential. Due to complexity of the problem, the theoretical studies of the influence of the geometry of the sample (existence of the constrictions or notches) on the DW depinning by a spin-polarized current are restricted by the micromagnetic simulations (see, e.g., recent publications[20,21]).

The knowledge of the behavior of the DW in artificially created structural defects and constrictions is extremely important for producing reliable memory devices. In spite of a growing number of experimental studies which gain insight into the properties of the DWs pinned by artificial defects (see, e.g., Refs. 11 and 22–25), a detailed understanding of the role of the shape effects on the dynamics of the DW driven by magnetic field and (or) spin-polarized current is still lacking.

 

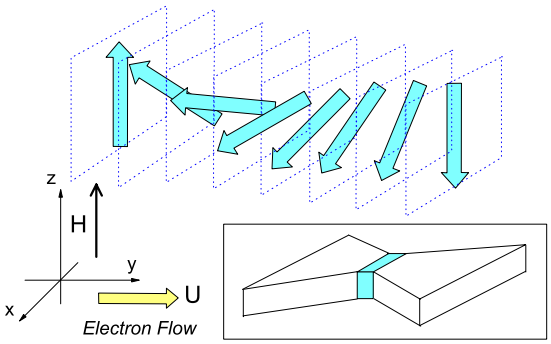


FIG. 1. (Color online) 180° Bloch domain wall. The magnetization in the domains are parallel and antiparallel along the $z$ axis (the easy axis). Inside the domain wall the magnetization rotates in the $xz$ plane. The low panel shows an example of constricted sample with the DW located in the constriction.

In this paper we study shape-dependent effects on the properties of DW confined in potential wells created by the defects in the bulk and by the variation in the sample shape (geometrical pinning). We analyze the difference in the depinning of the DW driven by applied magnetic field, from one side, and spin-polarized current, from another. The results of our studies are in accordance with the recent data and micromagnetic simulations of Refs. 20 and 21. We provide a plausible explanation of recent experimental data on manipulation of DW in constricted stripes of $SrRuO_3$.[11]

## II. GEOMETRY AND BASIC EQUATIONS

The DW displacement under driving magnetic field and spin-polarized current can be adequately described by Landau-Lifschitz-Gilbert equations complemented by a spin-transfer torque, $\tau_J$

$$\partial_t \mathbf{m} = -\gamma[\mathbf{m}\times\mathbf{H}_e] + \alpha[\mathbf{m}\times\partial_t\mathbf{m}] + \tau_J, \tag{1}$$

where $\gamma$ is the gyromagnetic ratio ($\gamma>0$), $\alpha$ is the dissipation parameter, $\mathbf{H}_e=-\delta F/\delta\mathbf{M}$ is effective magnetic field, $F$ is free energy density of the ferromagnet, and $\mathbf{m}=\mathbf{M}/M_s$ is a unit vector in the direction of the magnetization $\mathbf{M}$ ($M_s$ is the saturation magnetization).

Despite different approaches in calculation of the spin-transfer torque $\tau_J$, there is a consensus about the existence of adiabatic and nonadiabatic terms (or $\beta$ term[6]) that contribute to the spin-transfer torque

$$\tau_J = -(\mathbf{U}\cdot\nabla)\mathbf{m} + \beta\mathbf{m}\times(\mathbf{U}\cdot\nabla)\mathbf{m}, \tag{2}$$

where $\mathbf{U}=U\mathbf{n}$, $U=\mu_B JP/eM_s$ ($\mu_B$ is Bohr magneton, $e$ is the elementary charge, $J=\mathcal{I}/\mathcal{A}$ is the current *density*, $\mathcal{I}$ is a value of the current, $\mathcal{A}$ is a cross-section area of the sample, and $P$ is the spin polarization), $\mathbf{n}$ is unit vector in the direction of the current. Parameter $\beta$ is a ratio between the values of nonadiabatic and adiabatic torques.

Let us consider the 180° DW of Bloch type in a constricted platelike sample with variable size $L_x=L_x(y)\equiv L_0[1+\mathcal{G}(y)]$ along $x$ direction and constant dimensions $L_y$ and $L_z$ along $y$ and $z$ axis as shown in Fig. 1. The function $\mathcal{G}=\mathcal{G}(y)$ describes the change in the sample shape. In the absence of the constriction $\mathcal{G}=0$ and $L_x=L_0$. The DW width, $\Delta$, is much less than the width of the plate, $L_z$, i.e., $\Delta\ll L_z$. The surface of the sample is parallel to the $xy$ plane, and the domain wall, being parallel to the $xz$ plane, separates two domains with magnetization $M(y)$ along the $+z$ or $-z$ direction and is located initially in the constriction at $y=0$.

The free energy functional of the ferromagnet is $\mathcal{F}=\int_V \mathbf{dr}F$ where the free energy density $F=F[\mathbf{m}(\mathbf{r}),\partial\mathbf{m}(\mathbf{r})/\partial x_i]$ is defined by

$$F = K[-m_z^2 + qm_y^2 + \Delta_0^2(\partial_i m_j)(\partial_i m_j)] - HM_s m_z. \tag{3}$$

Here the first and second terms in square brackets describe the magnetic crystallographic anisotropy, the third term is the exchange energy, and the last term is the Zeeman energy in an external magnetic field $\mathbf{H}\|\mathbf{z}$. In Eq. (3) $K>0$ is the parameter of the easy-axis crystallographic anisotropy, the ratio $q=K_\perp/2K>0$ determines a joint effect of orthorhombic anisotropy and the magnetostatic energy, and $\Delta_0$ is a half-width of the DW at rest, which characterizes the stiffness of the spin system. The choice of the sign $q>0$ implies alignment of the magnetization $\mathbf{M}$ in the $xz$ plane. Thus, in the absence of the driving force the formation of DW of Bloch type with the rotation of the magnetization in $xz$ plane is energetically more favorable.

The magnetization $\mathbf{m}$ can be expressed in polar coordinates, $\mathbf{m}=(\sin\theta\cos\phi,\sin\theta\sin\phi,\cos\theta)$. In the absence of driving forces ($\mathbf{H},\mathbf{U}=0$) the ground state of the system is defined by minimization of the free energy with respect to azimuthal, $\phi$, and polar, $\theta$, angles, i.e., $\delta\mathcal{F}/\delta\phi=0$ and $\delta\mathcal{F}/\delta\theta=0$. This yields the well-known structure of Bloch DW located at the center of the sample constriction ($y=0$): $\theta_0=2\tan^{-1}\exp(y/\Delta_0)$ and $\phi_0=0$.

The standard approach in statics and dynamics of the DW is to use the Slonczewski equations for two canonically conjugated variables, the coordinate of the center of the DW $\eta$, and azimuthal angle $\phi$ (see, e.g., Ref. 13), which are independent of the coordinate $y$. For a sample with variable cross-section area $\mathcal{A}(y)=\mathcal{A}_0[1+\mathcal{G}(y)]$ [$\mathcal{A}_0=L_zL_0$ is the area of the cross section at $y=0$, and $\mathcal{G}(\eta)$ is a shape function dependent on the geometry of the sample] these equations are

$$\left(\frac{d\phi}{dt}+\frac{\alpha}{\Delta}\frac{d\eta}{dt}\right)[1+\mathcal{G}(\eta)] = -\frac{\gamma}{2M_s}\frac{\delta\sigma}{\delta\eta}+\beta\frac{U_0}{\Delta},$$

$$\left(\frac{d\eta}{dt}-\alpha\Delta\frac{d\phi}{dt}\right)[1+\mathcal{G}(\eta)] = \frac{\gamma}{2M_s}\frac{\delta\sigma}{\delta\phi}+U_0, \tag{4}$$

where $U_0=[1+\mathcal{G}(y)]U(y)$, $\Delta=\Delta_0(1+q\sin^2\phi)^{-1/2}$ is the effective DW width, and $\sigma(\eta,\phi)$ is the surface energy of the DW determined by the integral across the whole DW width

$$\sigma = \mathcal{A}_0\int dy[1+\mathcal{G}(y)]F[\theta_0(y-\eta),\phi]. \tag{5}$$

The goal of the present work is not investigation of the DW motion but determination of the depinning threshold, when such motion becomes possible. Therefore, one may ignore the time dependence of the variables. The second term $\propto\beta$ in the spin torque (nonadiabatic torque), Eq. (2), is most rel-

evant for depinning. This term is related to the momentum transfer between the polarized current and the DW. The adiabatic torque [the first term in Eq. (2)] causes the rotation of the DW plane around $z$ axis relative to it equilibrium position ($xz$ plane) but does not affect the DW depinning directly.

## III. DEPINNING OF DOMAIN WALLS

Usually, the pinning (coercivity) force on a DW originates from randomly located defects, which create potential wells for the DW in the sample bulk. However, key features of the bulk pinning phenomenon can be investigated using a simpler model of a DW in a periodic potential. The latter enters the DW surface energy, i.e., $\sigma \rightarrow \sigma + \sigma_p$ with $\sigma_p = 2H_p M_s [1+\mathcal{G}(\eta)]\xi f(\eta)$, where $f(\eta+2\xi)=f(\eta)$ is a periodic function with a period $2\xi$. Within the period $(-\xi \leq \eta \leq \xi)$ this function can be approximated by a parabolic function $f(\eta) = (1/2)(\eta/\xi)^2$. In addition to the pinning on the defects, there is another type of pinning (geometrical pinning) related to the change in the sample shape. Eventually neglecting the structure of the DW, i.e., assuming that $\sin^2\theta(y) = 2\Delta\delta(y)$, from Eq. (4) with use of Eq. (5) we obtain

$$\beta \frac{U_0}{1+\mathcal{G}(\eta)} + \gamma H \Delta = \gamma H_a \Delta_0^2 \frac{\partial_\eta \mathcal{G}(\eta)}{1+\mathcal{G}(\eta)} + \gamma H_p \xi \partial_\eta f(\eta)\Delta,$$

$$\frac{U_0}{1+\mathcal{G}(\eta)} = -\frac{q}{2}\gamma H_a \Delta \sin 2\phi, \tag{6}$$

where $H_a = 2K/M_s$ is a magnetic field corresponding to the easy-axis magnetic crystallographic anisotropy of a sample. According to Eq. (6), the modulation of the sample width gives rise to an effective geometrical pinning of the DW. It follows from Eqs. (6) that DW can be depinned by action of magnetic field, $H$, or the nonadiabatic contribution of the spin-polarized current, $\beta \neq 0$. In the following, we consider two particular cases, $H \neq 0$, $U=0$ and $U \neq 0$, $H=0$.

### A. Depinning by applied magnetic field: $H \neq 0$, $U=0$

In case of $H \neq 0$ and $U=0$, it follows from Eq. (6), that $\phi=0$, $\Delta=\Delta_0$, and the depinning of the DW by magnetic field is not affected by the presence of the orthorhombic anisotropy. Thus, instead of the first equation in Eq. (6) we have

$$[H - H_p \xi \partial_\eta f(\eta)][1+\mathcal{G}(\eta)] - H_a \Delta_0 \partial_\eta \mathcal{G}(\eta) = 0. \tag{7}$$

Equation (7) manifests the absence of a total force experienced by DW. The driving force from the magnetic field (the term $\propto H$) and the bulk pinning force confining the DW in a potential well (the term $\propto H_p$) are proportional to the total DW area, $\sim[1+\mathcal{G}(\eta)]$ while the force experienced by the DW in a shape-dependent pinning potential is determined by the derivative of the shape function $\partial_\eta \mathcal{G}(\eta)$ [the last term in Eq. (7)].

For simple shape potential, which can be expanded in series on DW displacement $\eta$, the function $\partial_\eta \mathcal{G}(\eta)/[1+\mathcal{G}(\eta)]$ reaches a maximum at some value of the parameter $\eta=\zeta$. Thus, it is insightful to characterize the geometric pinning potential, which is responsible for the shape effect, by the strength of the potential $H_\zeta$ and the characteristic distance $\zeta$, which are analogous to the parameters $H_p$ and $\xi$ of the pinning potential due to the defects. The value of the critical magnetic field $H_\zeta$ is defined by

$$H_\zeta = \max\left\{ H_a \Delta_0 \frac{\partial_\eta \mathcal{G}(\eta)}{1+\mathcal{G}(\eta)} \right\} = H_a \Delta_0 \frac{\partial_\zeta \mathcal{G}(\zeta)}{1+\mathcal{G}(\zeta)} \tag{8}$$

while $\zeta$ is obtained from the condition of a potential extremum $(1+\mathcal{G})\partial^2_{\zeta\zeta}\mathcal{G} - (\partial_\zeta \mathcal{G})^2 = 0$.

Thus, the presence of a constriction results in the change of the DW area and appearance of the geometrical pinning, which is independent of the distribution of defects. In absence of pinning on defects ($H_p=0$), the increase in the applied magnetic field below the critical field ($H < H_\zeta$) causes the DW displacement $\eta(H)$ (which is not a linear function of a magnetic field, in general) until its depinning at $H=H_\zeta$.

With use of $H_\zeta$ and $\zeta$ both terms that contribute to the DW pinning [see Eq. (7)] can be rewritten in a similar way

$$H - H_p \frac{\eta}{\xi}\Theta(\xi - |\eta|) - H_\zeta \psi(\eta)\Theta(\zeta - |\eta|) = 0, \tag{9}$$

where $\Theta(\xi)$ is a step function and the function $\psi(\eta)$ is defined according to

$$\psi(\eta) = \frac{\partial_\eta \mathcal{G}(\eta)[1+\mathcal{G}(\zeta)]}{\partial_\zeta \mathcal{G}(\zeta)[1+\mathcal{G}(\eta)]}. \tag{10}$$

Equation (9) defines a function $\eta = \eta(H)$ and can be solved for given geometry of the constriction. The results of numerical calculation of the function $\eta = \eta(H)$ in the particular case of a parabolic potential created by the constriction when $\mathcal{G} = (\eta/\zeta)^2$ are shown in Fig. 2 and reveal the general features of the DW depinning by the applied magnetic field $H$. Figure 2 illustrates the possibility of four different scenarios of DW depinning dependent on the relation between $\xi$ and $\zeta$, from one side, and $H_p$ and $H_\zeta$, from another. The analysis shows that these scenarios can be classified according to the values of two critical parameters, namely, the depinning magnetic field $H_c$ and critical value of the DW displacement $\eta_c$. The value of $H_c$ and $\eta_c$ are defined according to

$$H_c = \begin{cases} \max\{H_p; H_\zeta + (\zeta/\xi)H_p\} & \text{if } \zeta \leq \xi \\ \max\{H_\zeta; H_p + H_a\Delta_0 \partial_\xi \mathcal{G}(\xi)/[1+\mathcal{G}(\xi)]\} & \text{if } \zeta > \xi \end{cases} \tag{11}$$

and

$$\eta_c = \begin{cases} \xi & \text{if } H_c = H_p, H_p + H_a\Delta_0 \partial_\xi \mathcal{G}(\xi)/[1+\mathcal{G}(\xi)] \\ \zeta & \text{if } H_c = H_\zeta, H_\zeta + (\zeta/\xi)H_p, \end{cases} \tag{12}$$

where we assume that the maximum width of the constriction along $y$ axis exceeds the critical distance $\eta_c$. For $H \geq H_c$ $(\eta \geq \eta_c)$ the pinning potential cannot stop motion of the DW.

In Ref. 20 geometrically confined DWs are imaged directly with sub-10 nm resolution using off-axis electron holography and the magnetic fields needed to depin DWs from the constriction are measured as a function of the constric-

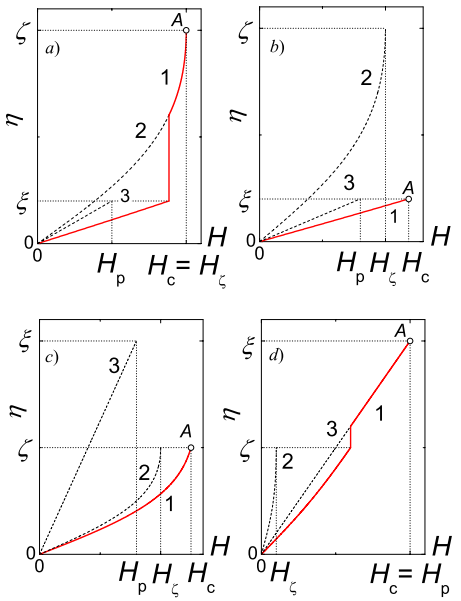


FIG. 2. (Color online) The plots $\eta = \eta(H)$, which illustrate four different scenarios for the depinning of the DW subjected to an applied magnetic field $H$, for [(a) and (b)] $\zeta > \xi$ and [(c) and (d)] $\zeta \leq \xi$, as described in the text. The solid curves 1 show the DW displacement $\eta$ for the joint effect of bulk pinning and geometrical pinning potentials. The DW displacement in the presence only of bulk pinning or geometric pinning is shown by dashed curves 2 and 3 respectively. The open circle corresponds to critical point $A(\eta_c, H_c)$, where eventually depinning takes place. The critical magnetic field $H_c$ and the critical displacement of the DW $\eta_c$ are defined by Eqs. (11) and (12).

tion width $w$ [see, Fig. 3(a)]. The value of magnetic field that is governed by the material imperfections and edge roughness (in a sample without constriction) is 60 Oe while the depinning field of the narrowest constriction is 335 Oe.

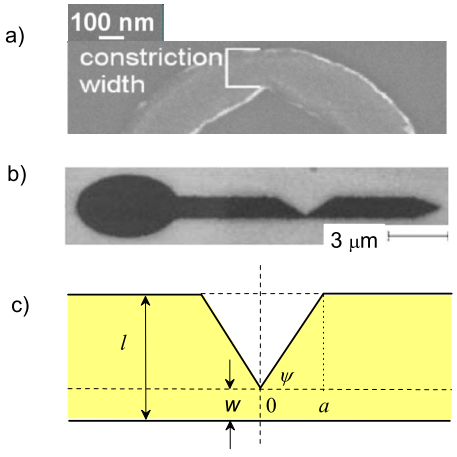


FIG. 3. (Color online) (a) Scanning electron microscope image (SEM) of a part of wide wavy line structure with a small notch (140 nm constriction) fabricated on permalloy ($Ni_{80}Fe_{20}$) structures (referred from Ref. 20), (b) SEM image of notch structure fabricated on $Si/SiO_2$ substrates using e-beam lithography and sputtering of $Ni_{80}Fe_{20}$(20 nm)/Au(1 nm) (referred from Ref. 21), and (c) the simulated shape of the constricted sample.

Therefore, the geometrically induced pinning is stronger than the pinning due to the sample defects. This enables the measuring of the dependence of the depinning field on the notch geometry. In the interval $|\eta| \leq a$, the shape function of the notch can be modeled by the linear function $\mathcal{G}(\eta) = (|\eta|/w)\tan\psi$, where $\psi$ is a notch angle [see, Fig. 3(c)]. At the conditions of the experiments,[20] it follows from Eqs. (11) and (12) that a critical value of magnetic field is $H_c = (\Delta_0/w)H_a \tan\psi$ and a critical value of the displacement of a DW is $\eta_c^{(H)} = \zeta = 0$, where the upper subscript shows that the critical displacement of a DW corresponds to the depinning in applied magnetic field. The critical magnetic field is scaled as inverse width of the notch, i.e., $H_c \sim w^{-1}$. This result has a simple physical meaning, i.e., the narrower the notch width is, the deeper is the potential to be overcome by a DW located at the notch. It is in accord with the data and numerical simulations of Ref. 20 which demonstrates the increase in depinning field, $H_c$ with decrease in constriction width, $w$.

### B. Depinning by a spin-polarized current: $U \neq 0$, $H = 0$

In the case of $U \neq 0$, $H = 0$, instead of Eq. (6) we have another pair of equations

$$\beta U_0 - \gamma H_a \Delta_0^2 \partial_\eta \mathcal{G}(\eta) - [1 + \mathcal{G}(\eta)]\gamma H_p \Delta \xi \partial_\eta f(\eta) = 0, \tag{13}$$

$$\frac{U_0}{1 + \mathcal{G}(\eta)} = -\frac{q}{2}\gamma H_a \Delta \sin 2\phi. \tag{14}$$

Equation (13) manifests the balance of forces on the DW: the forces from the spin-polarized current ($\sim\beta$) and the geometrical pinning ($\sim H_a$), and the bulk pinning force ($\sim H_p$). Equation (14) defines the function $\phi = \phi(\eta, U_0)$

$$\sin\phi = -\mathcal{U}\left\{\frac{1}{2}(1 - q\mathcal{U}^2) + \left[\frac{1}{4}(1 - q\mathcal{U}^2)^2 - \mathcal{U}^2\right]^{1/2}\right\}^{-1/2}, \tag{15}$$

where $\mathcal{U} = U_0/2q\gamma H_a \Delta_0[1 + \mathcal{G}(\eta)]$. Substituting Eq. (15) into Eq. (13) one can calculate the function $\eta = \eta(U_0)$. For the sake of simplicity we neglect the change in the DW width assuming that $\Delta \approx \Delta_0$, which is true if $\phi \ll 1$ ($\mathcal{U} \ll 1$). In this case Eq. (13) can be rewritten in a following way:

$$\frac{\beta U_0}{\gamma \Delta_0} - H_a \Delta_0 \partial_\eta \mathcal{G}(\eta) - [1 + \mathcal{G}(\eta)]H_p \xi \partial_\eta f(\eta) = 0. \tag{16}$$

It follows from Eq. (16), that in case of unconstricted sample ($\mathcal{G} = 0$) a DW can be depinned and participate in a steady-state motion when the current exceeds the critical value defined by the equation $\beta U_0^c / \gamma \Delta_0 = \max H_p \xi \partial_\eta f(\eta)$.

The condition for DW geometric depinning by the current is more severe than by the magnetic field. This because the pressure on the DW from the constant magnetic field (the force per unit area of the DW) does not depend on the DW area growing with the DW displacement, whereas the pressure from the constant current is determined by the current density, which is inversely proportional to the DW area. According to Eq. (16) at $H_p = 0$, the critical value of a current is

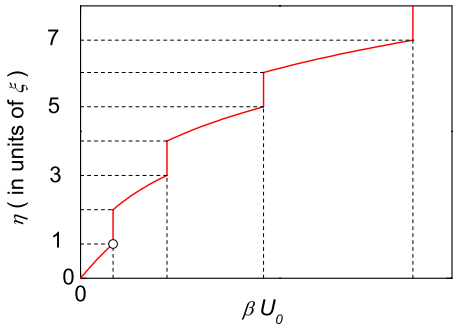


FIG. 4. (Color online) The plots $\eta=\eta(\beta U_0)$ of the DW confined in potential wells created by artificially fabricated constriction and bulk pinning centers. The jumps of the function $\eta=\eta(\beta U_0)$ are the result of the DW depinning from local volume defects within periods of the potential landscape. The values of the current-dependent parameter $\beta U_0$ required to depin the wall from the local potential are shown by the vertical dashed lines. The increase in the driving force results in a step-by-step drift of the DW. In calculations we use a parabolic shape function $\mathcal{G}=(\eta/\zeta)^2$. Open circle corresponds to the critical parameters for a sample without constriction. Note the absence of the depinning critical point for the constricted sample.

determined by the threshold $\beta U_0^{(g)}=\gamma H_a \Delta_0^2 \max\{\partial_\eta \mathcal{G}(\eta)\}$ above which the DW can overcome the geometrical pinning. For a parabolic shape function $\mathcal{G}=(\eta/\zeta)^2$, the function $\partial_\eta \mathcal{G}(\eta)$ is unbound, and DW depinning from the geometric pinning potential is impossible. Let us consider the DW behavior in this case.

We assume that a single DW is initially located in the constricted area ($\eta=0$). The increase of the current density above its critical value at a given position of the DW results in the drift of the DW from the constriction into expansion part of the sample. Such a drift is accompanied by the increase in the DW area followed by the decrease of the current *density* (the current does not depend on the location of the DW) below its critical value. As a result, the DW will be eventually pinned in a new position by an array of the nearest defects. The further increase in the current results in increase in a driving force and a displacement of the DW into a new position where the driving force is balanced by the increase in the pinning force. At this new position the DW is stuck again till the next increase of the current. Actually, in the presence of bulk pinning centers the displacement of the DW under spin-polarized current is characterized by a step-by-step drift over an array of bulk defects.

Equation (16) can be solved numerically for given functions $\mathcal{G}(\eta)$ and $f(\eta)$. The results of numerical calculation of the function $\eta=\eta(\beta U_0)$ for a parabolic shape function $\mathcal{G}=(\eta/\zeta)^2$ are present in Fig. 4 which illustrates the absence of the critical point on the curve $\eta=\eta(\beta U_0)$ ($\eta\to\infty$ when $\beta U_0\to\infty$), contrary to the case of depinning of a DW driven by a magnetic field $H$ (see Fig. 2).

Recently, the threshold current density required for depininnig a DW from a constriction with variable profile in nanowires was investigated in Ref. 21. A set of notched structures has been fabricated on $Si/SiO_2$ substrates using e-beam lithography technique and sputtering of $Ni_{80}Fe_{20}$(20 nm)/Au(1 nm) [see, Fig. 3(b)]. The variation in the threshold current on the notch angle, $\psi$, was measured, while the wire width, $l$, and constriction width, $w$, were kept fixed at $l=1.4$ $\mu$m and $w=500$ nm [Fig. 3(c)]. Using the same shape function, as in Sec. III A, i.e., $\mathcal{G}(\eta)=(|\eta|/w)\tan\psi$, and $f(\eta)=(1/2)(\eta/\xi)^2$, instead of Eq. (16) we have

$$\frac{\beta U_0}{\gamma\Delta_0}-H_a\frac{\Delta_0}{w}\tan\psi-\left(1+\frac{\eta}{w}\tan\psi\right)H_p\frac{\eta}{\xi}=0. \qquad (17)$$

For correct determination of a critical value of current density (current per cross-sectional area of nanowire), i.e., $J_c\sim\beta U_0 w/\gamma\Delta_0 l$, the relation between a geometrical pinning potential and a pinning potential governed by the imperfections of the sample is needed. Assuming for simplicity that the main contribution to the DW pinning is due to geometrical pinning and neglecting the contribution from the pinning on the defects which can be made due to location of a notch at a small part of the wire and is the case of the experiment in Ref. 21, one can obtain $J_c\sim\tan\psi$ and $\eta_c^{(J)}=0$ (see, Ref. 26). The increase in critical current density, $J_c$, with increase of the notch angle, $\psi$, has a simple explanation, the larger is the notch angle, the deeper is the pinning potential to overcome by the DW located at the center of the constriction. Therefore, the developed theory is consistent with the results[21] where the depinning threshold current was observed to vary almost linearly at the values of $\psi=21°$, 33°, 43°, and 53°.

### C. Domain wall in a constricted sample of $SrRuO_3$ and comparison with experiment

The developed theory can be exploited to understand the data on depinning of the DW from double V-shape constriction in submicroscopic patterns of $SrRuO_3$.[11] $SrRuO_3$ is a metallic perovskite with orthorhombic structure ($a=5.53$, $b=5.57$, $c=7.82$ Å) and an itinerant ferromagnet with Curie temperature of ~150 K and a saturated magnetization of $\sim 1.4\mu_B$ per ruthenium. It shows so-called bad metal behavior at high temperatures but is a Fermi liquid at low temperatures. $SrRuO_3$ exhibits a positive Seebeck coefficient in the wide range of the temperature from ~0 K till ~1000 K,[27,28] manifesting the holelike character of the charge carriers. The samples are high-quality epitaxial thin films of $SrRuO_3$ grown by reactive electron beam coevaporation on slightly miscut (~0.2°) $SrTiO_3$ substrates with the [001] and $[\bar{1}10]$ axes in the film plane. These films exhibit a large uniaxial magnetocrystalline anisotropy (anisotropy field $H_a\approx 10$ T at $T\to 0$ K) with the easy axis tilted out of the film (~45°) and with an in-plane projection along $[\bar{1}10]$. Consequently, the domain magnetization is out of film plane, the Bloch DWs are parallel to $[\bar{1}10]$ axis and the orthorhombic anisotropy (including the magnetostatic energy related to the shape anisotropy of the sample) contributes to the structure of the DW. Due to the large uniaxial magnetic anisotropy the DWs are relatively narrow with temperature independent width of ~3 nm.

The experimental setup is shown in Fig. 5(a). The measurements on the displacement of the DW driven by mag-

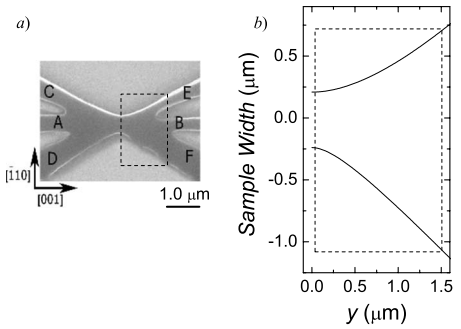


FIG. 5. (a) Scanning electron microscope image of the patterned sample Ref. 12) and (b) the shape function of the constricted sample. Current pulses are injected between A and B. The average magnetization is determined by measurement of extraordinary Hall effect between C and D and between A and B. The rectangle bounded by the dashed line shows the region of the sample where the DW experiences a geometric pinning.

netic field and spin-polarized current were performed on a high-quality 375-Å-thick film of $SrRuO_3$ with the resistivity ratio of 20 ($\sim 10$ $\mu\Omega$ cm at 4 K). The DW initially located at the constriction [see, Fig. 5(a)] was unpinned under the action of a magnetic field or a spin-polarized current and moved in the positive direction of $y$ axis (parallel to [001]) toward the pair of leads EF. The magnetic state of the sample in the region of contacts EF was monitored by measuring of extraordinary Hall effect (EHE) proportional to the average component of magnetization $M_z$ perpendicular to the film plane ($xy$ plane). The final location of the DW at the leads EF was deduced by the change of the sign of EHE followed by the change of the magnetic state at EF. The experiment shows that the DW displacement into a final position at the leads EF is achieved only with a value of the magnetic field (current density) above a certain threshold for the magnetic field or the current.

The shape of the sample [see Fig. 5(b)] can be approximated by a function

$$\mathcal{G}(\eta) = \frac{(\eta/\zeta_1)^2}{1+\eta/\zeta_2} + \frac{(\eta/\zeta_3)^2}{1+\eta/\zeta_4}, \tag{18}$$

where $\zeta_1 = 1.138$ $\mu$m, $\zeta_2 = 2.6$ $\mu$m, $\zeta_3 = 0.561$ $\mu$m, and $\zeta_4 = 0.52$ $\mu$m. The results of numerical calculation show that a function $G(\eta) = \partial_\eta \mathcal{G}(\eta)/[1+\mathcal{G}(\eta)]$ has a maximum at $\eta = \zeta = 0.44$ $\mu$m with $G(\zeta) = 1.1675$ $\mu\text{m}^{-1}$. The assumption $\xi \ll \zeta$, which is true assuming that $\xi \sim \Delta \sim 1.5$ nm, leaves two possibilities for the critical value of magnetic field $H_c$ [see Eq. (11)]

$$H_c = \max\left\{ H_\zeta; H_p + \frac{1}{2} H_a \xi \Delta \left( \frac{1}{\zeta_1^2} + \frac{1}{\zeta_3^2} \right) \right\}, \tag{19}$$

where we use $\mathcal{G}(\eta) \approx \eta^2(\zeta_1)^{-2} + \zeta_1)^{-2}$ for $\eta \sim \xi$. The choice of $H_c$ in Eq. (19) depends on the critical value of magnetic field corresponding to the geometrical pinning $H_\zeta$ given by Eq. (8). Using the values of $H_a \sim 10$ T and $\Delta_0 \sim 1.5$ nm,[11] we obtain $H_\zeta \sim 160$ Oe, which is less than the highest value of the depinning field $H_c = 500$ Oe measured at the temperature $T = 40$ K.[11] Therefore, we conclude that the critical magnetic field measured in Ref. 11 is dominated by the contribution of bulk pinning on defects, i.e., $H_c \approx H_p$, in accordance with the conclusions of Ref. 11. Evaluating the critical field $H_c$ in Eq. (19), we have neglected the small contribution of $(\xi\Delta/2\zeta^2)H_\zeta$, which is on the order of several oersteds. It follows from Eq. (12) that the critical value of the DW displacement $\eta$ is $\xi \sim \Delta_0 = 1.5$ nm $\ll \zeta = 0.44$ $\mu$m, therefore the scenario illustrated in Fig. 2(b) is realized. After depinning when $H \geq H_\xi$ and $\eta \geq \xi \sim \Delta_0 = 1.5$ nm the DW moves freely (see Ref. 6) till it reaches the leads EF [Fig. 5(a)].

In case of current driven DW motion the measured value of a spin-polarized current corresponds to the arriving of the DW at the leads EF [see Fig. 5(a)]. Both contributions to the DW pinning resulting from the distribution of the defects and the change of the sample shape can be evaluated from the data[11] by use of Eq. (16). To calculate the value of the current predicted by the theory we replace $\xi\partial_\eta f(\eta)$ in Eq. (16) by its maximum value: $\max\{\xi\partial_\eta f(\eta)\} = 1$

$$\frac{\beta U_0}{\gamma \Delta_0} - H_a \Delta_0 \partial_\eta \mathcal{G}(\eta) - [1+\mathcal{G}(\eta)] H_p = 0. \tag{20}$$

Furthermore, we assume that the DW moves at the distance $\eta \approx 1.5$ $\mu$m till it is registered by observation of the change of the sign of extraordinary Hall effect at the leads EF (see, Fig. 5(a)). With use of $H_a \approx 10$ T, $\Delta_0 = 1.5$ nm and the measured value of the depinning field $H_p = 571$ Oe at $T = 40$ K (Ref. 11) one can show that $H_a \Delta_0 \partial_\eta \mathcal{G}(\eta) \approx 411$ Oe and $[1+\mathcal{G}(\eta)]H_p \approx 2250$ Oe which gives a relative contribution of the geometrical pinning $\sim 20\%$. The measurement of the corresponding current density allows to evaluate the parameter of the nonadiabaticity $\beta$. For $SrRuO_3$, the current density $J$ translates into the velocity $U_0$ according to $U_0[\text{m/s}] = 3.64 \times 10^{-10}$ $PJ[\text{A/m}]$. Substituting the measured value of the current density $J = 5.8 \times 10^{10}$ $\text{A/m}^2$ into Eq. (20) (Ref. 11) and using the value of spin polarization $P \approx 0.5$ (see Ref. 29) we obtain $\beta \approx 6$. Being in accord with the conclusions of the high efficiency of monitoring of the DW by spin-polarized current in $SrRuO_3$,[11] such large value of $\beta$ cannot be explained by the contribution of the spin-relaxation process, which gives the value of $\beta \sim \alpha \ll 1$ (see Refs. 7 and 8), but can be understood due to the dominant role of the reflection of the charge carriers from thin DWs in the framework of the theory developed in Ref. 6.

Since bulk pinning on defects varies from a sample to sample, it is unpractical to look for quantitative comparison of the theory and the experiment in the case of predominantly bulk pinning. However, if there are data for the critical magnetic field and the critical current for the *same* sample, one may easily find from the theory their ratio and compare it with the experimental values. As it was shown by Tatara and Kohno[6] the dynamics of the abrupt DW in ideal plate-parallel sample is dominated by the momentum transfer from the charge current to the DW via reflection of charge carriers from the DW. Since this momentum transfer determines also the DW contribution to the resistance, in accordance with Ref. 6 the parameter $\beta$ can be found from the relation

$$\frac{\beta U_0}{\gamma \Delta_0} = \frac{enR_w \mathcal{A}}{2M_s} J, \tag{21}$$

where $n$ is a total charge carrier density and $R_w$ is the DW contribution to the resistance. Substituting Eq. (21) into Eq. (16), we arrive at the equation that defines the value of the current density $J$ as a function of the displacement of the DW in the presence of bulk and geometric pinning. As was pointed out in Sec. III B, complete depinning of the DW from the potential produced by growing cross section of the sample is impossible. However, one may introduce the critical current density $J_c$ (determined at the constriction), at which the DW reaches the position where the DW is detected [the leads EF in Fig. 5(a)]. Then

$$J_c = J_{c0}[1 + \mathcal{G}(\eta)]\left[1 + \frac{H_a}{H_c}\frac{\Delta_0 \partial_\eta \mathcal{G}(\eta)}{1 + \mathcal{G}(\eta)}\right], \tag{22}$$

where $\eta$ is the distance between the sample constriction and the place of DW detection, and

$$J_{c0} = \frac{2M_s H_c}{en\mathcal{A}_0 R_w} \tag{23}$$

is the critical current density of depinning for the DW in an unconstricted sample.

The temperature dependent saturation magnetization $M_s = M_s(T)$ and the DW resistance $R_w$ were measured in Refs. 30 and 11, respectively. According to Ref. 11 the carrier density $n$ is about $1.6 \times 10^{28}$ $[1/\mathrm{m}^3]$. This offers an opportunity to compare the developed theory with the data.[11] Calculating the critical current density $J_c$ with help of Eq. (22), we assume that the relative contribution of the geometric pinning [the term $\propto H_a$ in Eq. (22)] is temperature independent and equals to the value of ~20% calculated at $T=40$ K. Then Eq. (22) yields $J_c \approx 5J_{c0}$. Figure 6 shows the experimentally determined critical current density (circles) together with the prediction of the theory using the experimentally found critical magnetic fields and taking into account the shape-dependent effect (geometric pinning). The figure illustrates a satisfactory agreement between the experiment and the theory.

It is important to note that the sign of the ratio between the current and the DW displacement depends on the sign of charge carriers. The relative sign of the current and the displacement in the experiment gives evidence that charge carriers are holes. This agrees with the experiment on the Seebeck effect.[27]

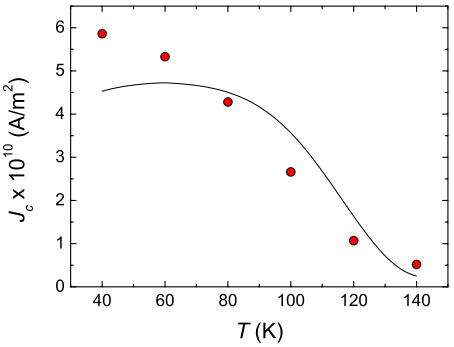


FIG. 6. (Color online) Temperature dependence of the critical current density for constricted sample $SrRuO_3$ (solid line) calculated using experimental values of the critical magnetic field and taking into account the shape effect. The measured current densities (circles) are the data from Ref. 11.

## IV. CONCLUSIONS

We investigated pinning of a domain wall by potentials produced by bulk defects and the sample shape. The process of depinning by an external magnetic field and by a spin-polarized current was analyzed. The shape-dependent pinning potential (geometric pinning) can essentially affect the process of depinning and may even make complete depinning by the spin-polarized current impossible. Though the absolute values of the critical magnetic fields and the critical currents, at which depinning occurs, are sample dependent and difficult for theoretical prediction, their ratio must be sample independent[6] and allows reliable comparison of the theory and the experiment. We performed this comparison and found a satisfactory agreement.

## ACKNOWLEDGMENTS

We appreciate the useful discussions with L. Klein. This work has been supported by the grants of the Israel Science Foundation founded by the Israel Academy of Sciences and Humanities (Grants No. 499/07 and No. 610/08).

*logoboy@phys.huji.ac.il

[1] C. H. Marrows, Adv. Phys. **54**, 585 (2005).
[2] L. Thomas, M. Hayashi, X. Jiang, R. Moriya, C. Rettner, and S. S. P. Parkin, Nature (London) **443**, 197 (2006).
[3] L. Berger, Phys. Rev. B **54**, 9353 (1996); L. Berger, *ibid.* **73**, 014407 (2006).
[4] J. C. Slonczewski, J. Magn. Magn. Mater. **159**, L1 (1996).
[5] Z. Li and S. Zhang, Phys. Rev. B **70**, 024417 (2004).
[6] G. Tatara and H. Kohno, Phys. Rev. Lett. **92**, 086601 (2004); G. Tatara, H. Kohno, and J. Shibata, J. Phys. Soc. Jpn. **77**, 031003 (2008); G. Tatara, H. Kohnoc, and J. Shibata, Phys. Rep. **468**, 213 (2008).
[7] A. Thiaville, Y. Nakatani, J. Miltat, and N. Vernier, J. Appl. Phys. **95**, 7049 (2004); A. Thiaville, Y. Nakatani, J. Miltat, and Y. Suzuki, Europhys. Lett. **69**, 990 (2005).
[8] S. Zhang and Z. Li, Phys. Rev. Lett. **93**, 127204 (2004).
[9] S. E. Barnes and S. Maekawa, Phys. Rev. Lett. **95**, 107204 (2005).
[10] O. Boulle, J. Kimling, P. Warnicke, M. Kläui, U. Rüdiger, G. Malinowski, H. J. M. Swagten, B. Koopmans, C. Ulysse, and G.

Faini, Phys. Rev. Lett. **101**, 216601 (2008).
[11] M. Feigenson, J. W. Reiner, and L. Klein, Phys. Rev. Lett. **98**, 247204 (2007).
[12] M. Feigenson, J. W. Reiner, and L. Klein, J. Appl. Phys. **103**, 07E741 (2008).
[13] A. P. Malozemoff and J. C. Slonczewski, *Magnetic Domain Walls in Bubble Materials* (Academic, New York, 1976).
[14] N. L. Schryer and L. R. Walker, J. Appl. Phys. **45**, 5406 (1974).
[15] L. R. Walker (unpublished); the calculation is reproduced by J. F. Dillon Jr., in *Treatise on Magnetism*, edited by G. T. Rado and H. Suhl (Academic, New York, 1963), Vol. III, p. 450.
[16] H. C. Bourne and D. S. Bartran, IEEE Trans. Magn. **10**, 1081 (1974).
[17] J. C. Slonczewski, J. Appl. Phys. **44**, 1759 (1973).
[18] S. S. P. Parkin, M. Hayashi, and L. Thomas, Science **320**, 190 (2008).
[19] P. Bruno, Phys. Rev. Lett. **83**, 2425 (1999).
[20] M. Kläui, C. A. F. Vaz, J. Rothman, J. A. C. Bland, W. Wernsdorfer, G. Faini, and E. Cambril, Phys. Rev. Lett. **90**, 097202 (2003); M. Kläui, H. Ehrke, U. Rüdiger, T. Kasama, R. E. Dunin-Borkowski, D. Backes, L. J. Heyderman, C. A. F. Vaz, J. A. C. Bland, G. Faini, E. Cambril, and W. Wernsdorfer, Appl. Phys. Lett. **87**, 102509 (2005).
[21] S. Lepadatu, A. Vanhaverbeke, D. Atkinson, R. Allenspach, and C. H. Marrows, Phys. Rev. Lett. **102**, 127203 (2009).
[22] L. K. Bogart and D. Atkinson, K. OShea, D. McGrouther, and S. McVitie, Phys. Rev. B **79**, 054414 (2009).
[23] D. Petit, A.-V. Jausovec, H. T. Zeng, E. Lewis, L. O'Brien, D. Read, and R. P. Cowburn, Phys. Rev. B **79**, 214405 (2009).
[24] A. Kunz and S. C. Reiff, Appl. Phys. Lett. **94**, 192504 (2009).
[25] S.-M. Moon, K.-W. Moon, D.-H. Kim, and S.-B. Choe, Appl. Phys. Lett. **95**, 013507 (2009).
[26] A pinning potential governed by the imperfections of the sample does not contribute to the pinning, if the enaquality $(H_a/H_p)\tan^2\psi \geq l(l-w)/\xi\Delta_0$ is fulfilled. In opposite case, the depinning current density is defined entirely by the imperfections of the sample, i.e., $J_c \sim H_p$ and $\eta_c^{(J)} = (l-w)\cot\psi$.
[27] Y. Klein, S. Hebért, A. Maignan, S. Kolesnik, T. Maxwell, and B. Dabrowski, Phys. Rev. B **73**, 052412 (2006).
[28] T. Maekawa, K. Kurosaki, H. Muta, M. Uno, and S. Yamanaka, J. Alloys Compd. **387**, 56 (2005).
[29] B. Nadgorny, M. S. Osofsky, D. J. Singh, G. T. Woods, R. J. Soulen, Jr., M. K. Lee, S. D. Bu, and C. B. Eom, Appl. Phys. Lett. **82**, 427 (2003).
[30] L. Klein, J. S. Dodge, T. H. Geballe, A. Kapitulnik, A. F. Marshall, L. Antognazza, and K. Char, Appl. Phys. Lett. **66**, 2427 (1995).